

Electron Dynamics in Solids

Shigeji Fujita¹, James McNabb III¹, Akira Suzuki²

¹Department of Physics, University at Buffalo, State University of New York, Buffalo, USA

²Department of Physics, Faculty of Science, Tokyo University of Science, Tokyo, Japan

Email: asuzuki@rs.kagu.tus.ac.jp

Received 30 January 2015; accepted 10 May 2015; published 13 May 2015

Copyright © 2015 by authors and Scientific Research Publishing Inc.

This work is licensed under the Creative Commons Attribution International License (CC BY).

<http://creativecommons.org/licenses/by/4.0/>



Open Access

Abstract

Following Ashcroft and Mermin, the conduction electrons (“electrons” or “holes”) are assumed to move as wave packets. Dirac’s theorem states that the quantum wave packets representing massive particles always move, following the classical mechanical laws of motion. It is shown here that the conduction electron in an orthorhombic crystal moves classically if the primitive rectangular-box unit cell is chosen as the wave packet, the condition requiring that the particle density is constant within the cell. All crystal systems except the triclinic system have k -vectors and energy bands. Materials are conducting if the Fermi energy falls on the energy bands. Energy bands and gaps are calculated by using the Kronig-Penny model and its 3D extension. The metal-insulator transition in VO_2 is a transition between conductors having three-dimensional and one-dimensional k -vectors.

Keywords

Electron Dynamics, Dirac’s Theorem, Primitive Rectangular-Box Unit Cell, Wave Packet, k -Vector

1. Introduction

Following Ashcroft and Mermin [1], we regard the conduction electron (“electron” or “hole”) as a wave packet. Dirac showed in his classic book [2] *Principles of Quantum Mechanics* that, the quantum wave packet moves, following classical mechanical laws. Dirac’s theorem is distinct from Ehrenfest’s theorem [3] that the quantum average of a dynamical variable follows a classical mechanical’s law of motion. Dirac’s theorem requires a unit cell. We shall show in the present work that if we regard the rectangular-box unit cell for the orthorhombic (ORC) crystal as the wave packet, then the “electron” (“hole”) moves, following the classical equations of motion.

In simple cubic (SC), tetragonal (TET) and orthorhombic (ORC) crystals, the lattices have natural orthogonal axes. Their unit cells are different only in having one (1), two (2) and three (3) different sides. Elements Po (Pa) form SC (TET) crystals.

In Section 2 an electron in electric and magnetic fields, a conduction electron in solids, and crystal lattice structures are introduced and summarized. In Section 3 a theory of electron dynamics for an ORC lattice is developed. Choosing the rectangular-box unit cell as the wave packet, we establish that there are 3D k -vectors. The results are summarized, using Bloch theorem [4]. In Section 4 energy bands and gaps are calculated for 1D and 3D Kronig-Penny models [5]. Summary and discussion are given in the final section.

2. Preliminaries

2.1. An Electron in Electromagnetic Fields

Let us take a classical electron in a free space moving in the electric field \mathbf{E} and a magnetic field \mathbf{B} . The Lorentz force \mathbf{F} is

$$\mathbf{F} = q(\mathbf{E} + \mathbf{v} \times \mathbf{B}), \quad (1)$$

where $q = -e$ is the charge and

$$\mathbf{v} = \frac{d\mathbf{r}}{dt} \equiv \dot{\mathbf{r}} \quad (2)$$

is the electron velocity. We introduce a vector potential \mathbf{A} and a scalar potential ϕ that generate the electric field \mathbf{E} and a magnetic field \mathbf{B} by

$$\mathbf{E} = -\nabla\phi - \frac{1}{c} \frac{\partial \mathbf{A}}{\partial t}, \quad (3)$$

$$\mathbf{B} = \nabla \times \mathbf{A}, \quad (4)$$

where

$$\nabla\phi \equiv \mathbf{i} \frac{\partial\phi}{\partial x} + \mathbf{j} \frac{\partial\phi}{\partial y} + \mathbf{k} \frac{\partial\phi}{\partial z} \quad (5)$$

$$\nabla \times \mathbf{A} \equiv \left(\frac{\partial A_y}{\partial z} - \frac{\partial A_z}{\partial y} \right) \mathbf{i} + \left(\frac{\partial A_z}{\partial x} - \frac{\partial A_x}{\partial z} \right) \mathbf{j} + \left(\frac{\partial A_x}{\partial y} - \frac{\partial A_y}{\partial x} \right) \mathbf{k}. \quad (6)$$

Note that the Cartesian coordinates (x, y, z) are used here. The del operator ∇ is undefined for non-orthogonal coordinates.

In Hamiltonian formulation a Hamiltonian H is defined:

$$H(\mathbf{r}, \mathbf{p}) = \frac{1}{2m} |\mathbf{p} - q\mathbf{A}(\mathbf{r}, t)|^2 + q\phi(\mathbf{r}, t). \quad (7)$$

The equations of motion are derived from

$$\dot{\mathbf{r}} = \frac{\partial H}{\partial \mathbf{p}}, \quad \dot{\mathbf{p}} = -\frac{\partial H}{\partial \mathbf{r}}. \quad (8)$$

We may quantize the dynamics by introducing the *fundamental commutation rules*:

$$[q_j, p_k] \equiv q_j p_k - p_k q_j = i\hbar; \quad [q_j, q_k] = [p_k, p_j] = 0, \quad (9)$$

where j and k indicate components: $(x, y, z) \equiv (q_1, q_2, q_3)$, $(p_x, p_y, p_z) \equiv (p_1, p_2, p_3)$.

2.2. A Conduction Electron

Wigner and Seitz used a primitive unit cell and lattice periodicity to obtain the ground-state energy of a metal [6]. Let us consider a conduction electron moving in a SC crystal. It is natural to choose the Cartesian coordinates

(x, y, z) along the cubic lattice axes. The unit cell is a cube with the side-length a , called the lattice constant. The ORC crystal has orthogonal axis with different side lengths: $a_1 \neq a_2$, $a_2 \neq a_3$, $a_3 \neq a_1$. The lattice potential $V(\mathbf{r}) \equiv V(x, y, z)$ is *lattice-periodic* if $V(\mathbf{r})$ is translation-invariant:

$$V(\mathbf{r}) = V(\mathbf{r} + \mathbf{R}), \quad (10)$$

where the *Bravais vector*

$$\mathbf{R} = la_1\mathbf{i} + ma_2\mathbf{j} + na_3\mathbf{k}, \quad (11)$$

is specified by integers-set (l, m, n) ; $l, m, n = \text{integers} = 0, \pm 1, \pm 2, \dots$.

The cubic cell may be chosen as the wave packet for the conduction electron. The center of mass of the wave packet is expected to move, following Hamilton's equation of motion. The rigorous proof will be given later. Following Ashcroft and Mermin, we may set up a model of electron dynamics in solids. It is necessary to introduce k -vectors:

$$\mathbf{k} = k_x\hat{e}_x + k_y\hat{e}_y + k_z\hat{e}_z, \quad (12)$$

where $\hat{e}_x, \hat{e}_y, \hat{e}_z$ are the orthonormal unit vectors, since k -vectors are involved in the equation of motion:

$$\hbar\dot{\mathbf{k}} \equiv \hbar\frac{d\mathbf{k}}{dt} = q(\mathbf{E} + \mathbf{v} \times \mathbf{B}), \quad (13)$$

where \mathbf{E} and \mathbf{B} are the electric and magnetic fields, respectively. The vector

$$\mathbf{v} = \frac{1}{\hbar} \frac{\partial \varepsilon}{\partial \mathbf{k}} \quad (14)$$

is the electron velocity, where $\varepsilon = \varepsilon(\mathbf{k})$ is the energy.

If an electron is in a continuous energy range (energy band), then it will be accelerated by the electric force, following Equation (13), and the material is a conductor. If the electron's energy is discrete and is in a forbidden band (energy gap), it does not move under a small electric force, and the material is an insulator. If the acceleration occurs only for a mean free time τ , that is, the inverse of the scattering frequency, the conductivity σ for a simple metal is given by Drude's formula [7]:

$$\sigma = q^2 n \tau / m^*, \quad (15)$$

where n is the electron density and m^* the effective mass.

For some crystals such as simple cubic (SC), face-centered-cubic (FCC), body-centered-cubic (BCC), tetragonal (TET) and ORC crystals, the choice of the orthogonal (x, y, z) -axis and the unit cells are obvious. The 2D crystals can also be treated similarly, only the z -component being dropped.

3. Theory

We assume that a wave packet is composed of superposable plane waves characterized by k -vectors. The superposability is the basic property of the Schrödinger wave function in free space. A monoclinic (MCL) crystal can be generated from a TET crystal by distorting the rectangular faces perpendicular to the c -axis into parallelograms. Material plane waves proceeding along the c -axis exist since the x - y planes containing atoms are periodic in the z -direction in equilibrium. It has then one-dimensional (1D) k -vectors. In the x - y plane there is an oblique net whose corners are occupied by V's for MCL (VO₂). The Bravais vector may be defined by

$$\mathbf{R}_{mm} = ma_1 + na_2, \quad (16)$$

where a_1 and a_2 are non-orthogonal base vectors. In the field theoretical formulation the field point \mathbf{r} is given by

$$\mathbf{r} = \mathbf{r}' + \mathbf{R}_{mm}, \quad (17)$$

where \mathbf{r}' is the point defined within the standard unit cell. Equation (16) describes the 2D lattice periodicity

but does *not* establish k -space as explained below.

To see this clearly, we first consider an electron in a simple square (SQ) lattice. The Schrödinger equation is

$$i\hbar \frac{\partial}{\partial t} \psi(\mathbf{r}) = -\frac{\hbar^2}{2m^*} \nabla^2 \psi(\mathbf{r}) + V(\mathbf{r})\psi(\mathbf{r}), \quad (18)$$

where the potential energy is periodic:

$$V(\mathbf{r}) = V(\mathbf{r} + \mathbf{R}_{mn}^{(0)}), \quad (19)$$

where $\mathbf{R}_{mn}^{(0)} \equiv ma_x + na_y = ma_1 e_x + na_2 e_y$. If we choose a set of Cartesian coordinates (x, y) , then the Laplacian term in Equation (18) is given by

$$\nabla^2 \psi(x, y) = \left(\frac{\partial^2}{\partial x^2} + \frac{\partial^2}{\partial y^2} \right) \psi(x, y), \quad (20)$$

a key step for the separation-of-variable method. If we choose a periodic square boundary with the side length Na (N : integer), then there are 2D Fourier transforms and (2D) k -vectors.

We now go back to the original rhombic system. If we choose the x -axis along either \mathbf{a}_1 or \mathbf{a}_2 , then the potential energy field $V(\mathbf{r}) = V(\mathbf{r} + \mathbf{R}_{mn})$ is *periodic* in the x -direction but it is *aperiodic* in the y -direction. For an infinite system the only acceptable boundary for the Fourier transformation is the periodic boundary condition. Hence there is *no* 2D k -space.

In SC, TET, and ORC crystals the lattices have natural orthogonal axes. We first take a rectangular 2D lattice. If the potential energy $V(x, y)$ is the sum of x - and y -dependent terms such that

$$V(x, y) = V_1(x) + V_2(y), \quad (21)$$

then the energy-eigenvalue Schrödinger equation:

$$-\frac{\hbar^2}{2m^*} \nabla^2 \psi(x, y) + [V_1(x) + V_2(y)]\psi(x, y) = E\psi(x, y), \quad (22)$$

where E is the energy, is separable:

$$\psi(x, y) = \psi_1(x)\psi_2(y). \quad (23)$$

The 1D Schrödinger equation in x is

$$\left[-\frac{\hbar^2}{2m^*} \frac{d^2}{dx^2} + V_1(x) \right] \psi_E(x) = E\psi_E(x), \quad (24)$$

where $V_1(x)$ is lattice-periodic:

$$V_1(x) = V_1(x + na) \quad \text{for} \quad -\infty < n (= \text{integers}) < \infty. \quad (25)$$

Clearly the wave function $\psi_E(x + na)$ also satisfies the same equation. Therefore, $\psi_E(x + na)$ is likely to be different from $\psi_E(x)$ only by an x -independent phase:

$$\psi_E(x + na) = e^{ikna} \psi_E(x), \quad (26)$$

where k is a real number, see below. Equation (26) represents a form of the *Bloch theorem* [4]. It generates far-reaching consequences in the theory of conduction electrons.

Let us discuss a few physical properties of the Bloch wave function ψ . By taking the absolute square of Equation (26), we obtain

$$|\psi(x + na)|^2 = |\psi(x)|^2. \quad (27)$$

The following three main properties are observed.

- The probability distribution function $P(x) \equiv |\psi(x)|^2$ is *lattice-periodic*:

$$P(x) \equiv |\psi(x)|^2 = P(x + na) \text{ for any } n. \quad (28)$$

- The exponential function of a complex number e^{iy} (y real) is periodic:

$$e^{iy} = e^{i(y+2\pi m)}.$$

where m is an integer. We may choose the real number k in Equation (26), called the k -number (2π times the wave number), to have a fundamental range:

$$-\frac{\pi}{a} < k < \frac{\pi}{a}; \quad (29)$$

the two end points are called the *Brillouin boundary* (points).

- There are a number of energy gaps (forbidden regions of energy) in which no solutions of Equation (24) exist. The energy eigenvalues E are characterized by the k -number and the zone number (band index) j , which enumerates the *energy bands*:

$$E = E_j(k). \quad (30)$$

This property (c) is not obvious, and it will be illustrated by examples later.

To further explore the nature of the Bloch wave function ψ , let us write,

$$\psi_E(x) = e^{ikx} u_{j,k}(x), \quad (31)$$

and substitute it into Equation (26). If the function $u_{j,k}(x)$ is lattice-periodic,

$$u_{j,k}(x) = u_{j,k}(x + na), \quad (32)$$

then Equation (26) is satisfied. Equation (31) represents a second form of the Bloch theorem. The Bloch wave function $\psi_E(x) = e^{ikx} u_{j,k}(x)$ has great similarity with the free-particle wave function:

$$\psi_{\text{free}}(x) = ce^{ikx}, \quad (33)$$

where c is a constant. The connection may be illustrated as follows.

For a free particle, the k -number can range from $-\infty$ to ∞ , and the energy is

$$E_{\text{free}} = \frac{p^2}{2m} \equiv \frac{\hbar^2 k^2}{2m} \quad (34)$$

with no gaps. These features are different from the properties (b) and (c).

An important similarity arises when we write the time-dependent wave function $\psi(x, t)$ in the running wave form:

$$\psi_E(x, t) = e^{i(kx - \omega t)} U(x) \quad (35)$$

where the frequency ω is defined by

$$\omega = \begin{cases} \hbar^{-1} E_j(k), & \text{for the Bloch electron;} \\ \hbar^{-1} E_{\text{free}}, & \text{for the free electron.} \end{cases} \quad (36)$$

and the amplitude $U(x)$ is defined by

$$U(x) = \begin{cases} u_{j,k}(x), & \text{for the Bloch electron;} \\ c, & \text{for the free electron.} \end{cases} \quad (37)$$

Equation (35) shows that the Bloch wave function $\psi_E(x)$ represents a running wave characterized by k -number k , angular frequency ω , and wave train $u_{j,k}(x)$.

The *group velocity* v of the Bloch wave packet is given by

$$v \equiv \frac{\partial \omega}{\partial k} = \frac{\partial E}{\partial k}. \quad (38)$$

By applying the (quantum) principle of wave-particle duality, we say that the Bloch electron moves with the *dispersion* (energy-momentum) *relation*:

$$E = \varepsilon_j(\hbar k) \equiv \varepsilon(p), \quad (39)$$

The velocity v is given by Equation (38). This gives a picture of great familiarity.

The lattice force $-dV/dx$ averaged over the unit cell is defined and calculated as

$$\begin{aligned} \left\langle -\frac{dV(x)}{dx} \right\rangle &\equiv \int_{-a/2}^{a/2} dx \left(-\frac{dV(x)}{dx} \right) \psi^*(x) \psi(x) \\ &= -V(x) \psi^*(x) \psi(x) \Big|_{-a/2}^{a/2} + \int_{-a/2}^{a/2} dx V(x) \frac{d}{dx} \psi^*(x) \psi(x), \end{aligned} \quad (40)$$

where the last line is obtained by partial integration. The first term on the right-hand side (r.h.s.) vanishes because both potential $V(x)$ and density $\psi^*(x)\psi(x)$ are periodic. When the unit cell is chosen as a wave packet, the minimum definition length of the density $\psi^*(x)\psi(x)$ is a . We may then assume that

$$\psi^*(x)\psi(x) = \text{constant}, \quad -\frac{a}{2} \leq x \leq \frac{a}{2}. \quad (41)$$

Using this, we obtain from Equation (40)

$$\left\langle -\frac{dV}{dx} \right\rangle = 0. \quad (42)$$

This property also holds for the y -motion. Extending these results to a 3D motion, we obtain the desired result:

$$\langle -\nabla V(\mathbf{r}) \rangle \equiv \int d^3r [-\nabla V(\mathbf{r})] \psi^*(\mathbf{r}) \psi(\mathbf{r}) = 0, \quad (43)$$

indicating that the conduction electron moves free from the lattice force. Only the external forces such as the electric and magnetic forces act on the conduction electrons.

Consider an infinite ORC lattice of lattice constants (a, b, c) . We choose a Cartesian frame of coordinates (x, y, z) along the lattice axes. The potential $V(x, y, z) = V(\mathbf{r})$ is lattice-periodic:

$$V(\mathbf{r}) = V(\mathbf{r} + \mathbf{R}) \quad (44)$$

where the Bravais lattice vector \mathbf{R} is defined by

$$\mathbf{R} \equiv n_1 a \mathbf{i} + n_2 b \mathbf{j} + n_3 c \mathbf{k} \quad (n_j \text{ are integers}). \quad (45)$$

The Schrödinger equation is

$$\left[-\frac{\hbar^2}{2m} \nabla^2 + V(\mathbf{r}) \right] \psi_E(\mathbf{r}) = E \psi_E(\mathbf{r}), \quad (46)$$

The Bloch wave function $\psi_E(\mathbf{r})$ satisfies

$$\psi_E(\mathbf{r} + \mathbf{R}) = e^{i\mathbf{k} \cdot \mathbf{R}} \psi_E(\mathbf{r}). \quad (47)$$

where $\mathbf{k} = (k_x, k_y, k_z)$ are k -vectors.

The three principal properties of the Bloch wave function are:

- The probability distribution $P(\mathbf{r})$ is lattice-periodic:

$$P(\mathbf{r}) \equiv |\psi(\mathbf{r})|^2 = P(\mathbf{r} + \mathbf{R}). \quad (48)$$

- The k -vector $\mathbf{k} = (k_x, k_y, k_z)$ has the fundamental ranges:

$$-\frac{\pi}{a} < k_x < \frac{\pi}{a}, \quad -\frac{\pi}{b} < k_y < \frac{\pi}{b}, \quad -\frac{\pi}{c} < k_z < \frac{\pi}{c}, \quad (49)$$

the end points, which form a rectangular box, are called the *Brillouin boundary*.

- The energy eigenvalues E have energy gaps, and the allowed energies E are characterized by the zone number j and the k -vectors:

$$E = \varepsilon_j(\hbar\mathbf{k}) \equiv \varepsilon_j(\mathbf{p}), \quad (50)$$

Using Equation (47), we can express the Bloch wave function ψ in the form:

$$\psi_E(\mathbf{r}) \equiv \psi_{j,\mathbf{k}}(\mathbf{r}) = e^{i\mathbf{k}\cdot\mathbf{r}} u_{j,\mathbf{k}}(\mathbf{r}), \quad u_{j,\mathbf{k}}(\mathbf{r} + \mathbf{R}) = u_{j,\mathbf{k}}(\mathbf{r}). \quad (51)$$

4. Energy Bands and Gaps

The Bloch energy-eigenvalues in general have bands and gaps. We show this by taking the *Kronig-Penny* (K-P) model [5]. Let us consider a periodic 1D square-well potential $V(x)$ with depth $V_0 (< 0)$ and well width $\beta \equiv a - \alpha$ as shown in **Figure 1**:

$$V(x) = \begin{cases} V_0, & \text{if } na - \beta < x < n\alpha, \\ 0, & \text{if } na < x < na + \alpha. \end{cases} \quad (52)$$

The Schrödinger equation can be written as in Equation (24). Since this is a linear homogeneous differential equation with constant coefficients, the wave function $\psi(x)$ should have the form:

$$\psi(x) = ce^{\gamma x}, \quad (c, \gamma \text{ are constants}). \quad (53)$$

According to the Bloch theorem, this function $\psi(x)$ can be written as

$$\psi_k(x) = e^{ikx} u_k(x), \quad (54)$$

$$u_k(x + a) = u_k(x), \quad (55)$$

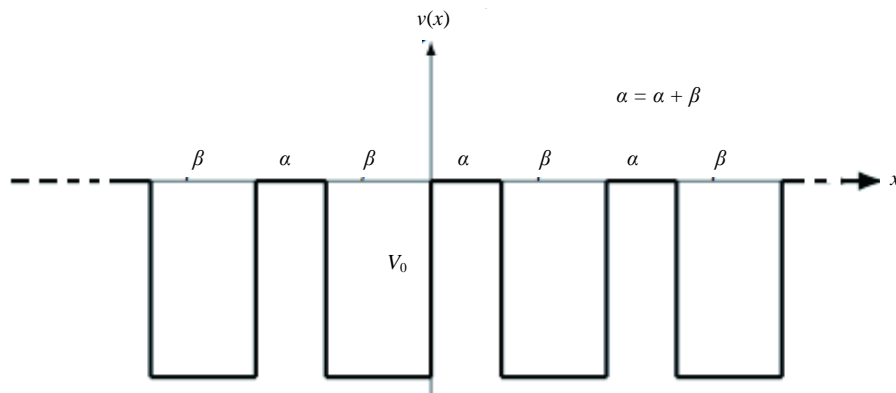


Figure 1. A Kronig-Penny potential has a square-well with depth V_0 and width β periodically arranged with period $a = \alpha + \beta$.

The condition that the function $\psi(x)$ be *continuous* and *analytic* at the well boundary yields the following relationships: [8]

$$\cos ka = \cosh K\alpha \cos \mu\beta + \frac{K^2 - \mu^2}{2K\mu} \sinh K\alpha \sin \mu\beta \equiv f(E), \tag{56}$$

$$E = \begin{cases} -\hbar^2 K^2 / (2m), & na < x < na + \alpha, \\ V_0 + \hbar^2 \mu^2 / (2m), & na - \beta \leq x \leq na, V_0 < 0. \end{cases} \tag{57}$$

By solving Equation (56) with Equation (57), we obtain the eigenvalue E as a function of k . The *band edges* are obtained from

$$f(E) = \pm 1, \tag{58}$$

which corresponds to the limits of $\cos ka$. Numerical studies of Equations (56) and (57) indicate that (1) there are, in general, a number of negative- and positive-energy bands; (2) at each band edge, an *effective mass* m^* can be defined, whose value can be positive or negative and whose absolute value can be greater or less than the electron mass m ; and (3) the effective mass is positive at the lower edge of each band, and it is negative at the upper edge. A typical dispersion relation for the model, showing energy bands and gaps, are shown in **Figure 2**.

At the lowest band edge ε_0 we have

$$f(\varepsilon_0) = 1. \tag{59}$$

Near this edge the dispersion (energy- k) relation calculated from Equation (56) is

$$\varepsilon = \varepsilon_0 + \frac{\hbar^2 k^2}{2m^*}, \quad (\varepsilon_0 < 0) \tag{60}$$

$$m^* \equiv -\hbar^2 a^{-2} f'(\varepsilon_0). \tag{61}$$

This one-dimensional K-P model can be used to study a simple 3D system. Let us take an ORC lattice of unit lengths (a_1, a_2, a_3) , with each lattice point representing a short-range attractive potential center (ion). The Schrödinger equation is hard to solve.

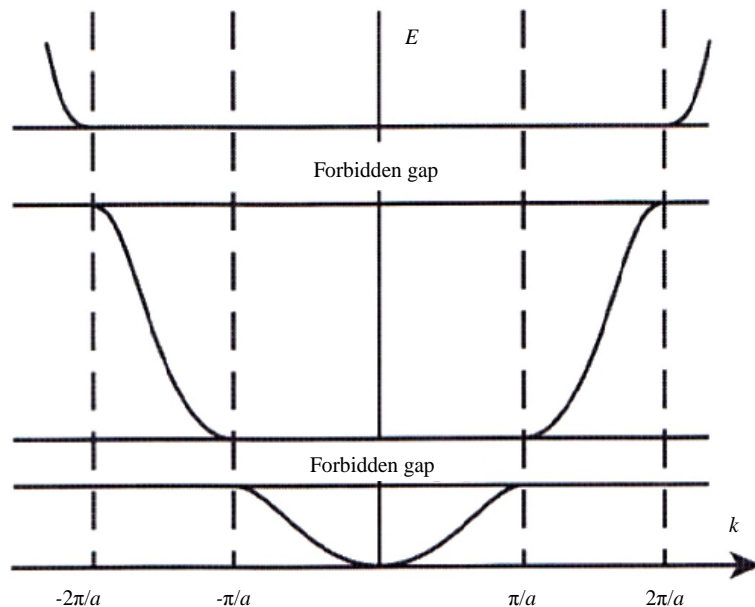


Figure 2. $E - k$ diagram showing energy bands and forbidden gaps.

Let us now construct a model potential V_s defined by

$$V_s(x, y, z) = V_1(x) + V_2(y) + V_3(z) \quad (62)$$

$$V_j(u) = \begin{cases} V_0 (< 0), & \text{if } na_j - \beta \leq u \leq na_j; \\ 0, & \text{otherwise.} \end{cases} \quad (63)$$

Here the n are integers. A similar two-dimensional model is shown in **Figure 3**. In 3D the domains in which $V_s \neq 0$ are parallel plates of thickness β ($< a_j$) separated by a_j in the direction x_j , $(x_1, x_2, x_3) \equiv (x, y, z)$. The intersection of any two plates are straight beams of cross section β^2 , where the potential V_s has the value $2V_0$. The intersections of three plates, where the potential V_s has the value $3V_0$, are cubes of side length β . The set of these cubes form an ORC lattice, a configuration similar to that of the commercially available molecular lattice model made up of balls and sticks. Note: Each square-well potential V_j has three parameters (V_0, β, a_j) , and this model represents the true potential fairly well [9]. The Schrödinger equation for the 3D model Hamiltonian

$$\begin{aligned} H_f &\equiv \frac{p_x^2 + p_y^2 + p_z^2}{2m} + V_1(x) + V_2(y) + V_3(z) \\ &= \frac{p_x^2}{2m} + V_1(x) + \frac{p_y^2}{2m} + V_2(y) + \frac{p_z^2}{2m} + V_3(z), \end{aligned} \quad (64)$$

can now be reduced to three 1D K-P equations. We can then write an expression for the energy of our model system near the lowest band edge as

$$E = \frac{\hbar^2}{2m_1} k_x^2 + \frac{\hbar^2}{2m_2} k_y^2 + \frac{\hbar^2}{2m_3} k_z^2 + \text{constant}, \quad (65)$$

where $\{m_j\}$ are effective masses.

Equation (65) is what is intuitively expected of the energy- k relation for the electron in the ORC lattice. It is stressed that we derived it from first principles, assuming a 3D model Hamiltonian H_s in Equations (62) and (63).

5. Discussion

5.1. The Coulomb Interaction

The Coulomb potential $V(|\mathbf{r}_1 - \mathbf{r}_2|)$ between two charges (q), located at \mathbf{r}_1 and \mathbf{r}_2 in vacuum is given by

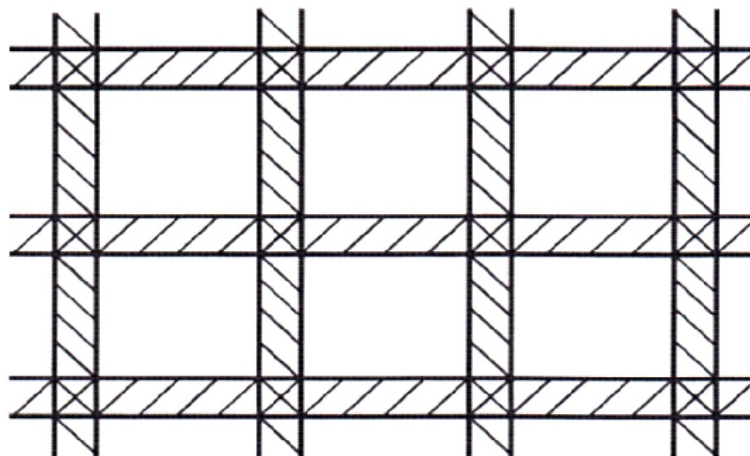


Figure 3. A 2D model potential. Each singly shaded stripe has a potential energy (depth) V_0 . Each cross-shaded square has a potential energy $2V_0$.

$$V(|\mathbf{r}_1 - \mathbf{r}_2|) \equiv V(r) = k \frac{q^2}{r}, \quad (66)$$

where $k = (4\pi\epsilon_0)^{-1}$ = Coulomb's constant, ϵ_0 = vacuum permittivity. Special relativity requires that the photon travels with the light speed c and no mass carrier can travel faster than c . Hence the instantaneous pair potential in Equation (66) is not allowed in relativistic quantum theory. In quantum electrodynamics the Coulomb interaction is discussed by means of the (longitudinal) photon exchange between two electrons and the zero-mass photon travels with the light speed c . Dirac's theorem [2] about particles as wave packets may be applied to this relativistic theory.

In classical statistical mechanics, a one-body distribution function $f(\mathbf{r}, \mathbf{p}, t)$ defined through

$$f(\mathbf{r}, \mathbf{p}, t) d^3 r d^3 p = \text{a relative probability of finding a particle in the phase space volume } d^3 r d^3 p. \quad (67)$$

is introduced. Integrating over the phase space we obtain

$$\iint d^3 r d^3 p f(\mathbf{r}, \mathbf{p}, t) = N = \text{number of particles}. \quad (68)$$

An electron gas system is characterized by the Hamiltonian

$$H = \sum_{j=1}^N \frac{p_j^2}{2m} + \frac{1}{2} \sum_{j=1}^N \sum_{k=1}^N V(|\mathbf{r}_j - \mathbf{r}_k|). \quad (69)$$

The evolution equation for f is

$$\frac{\partial f(\mathbf{r}, \mathbf{p}, t)}{\partial t} + \frac{\mathbf{p}}{m} \frac{\partial f}{\partial \mathbf{r}} = \iint d^3 r' d^3 p' \frac{\partial}{\partial \mathbf{r}} V(|\mathbf{r} - \mathbf{r}'|) \cdot \frac{\partial}{\partial \mathbf{p}} f_2(\mathbf{r}, \mathbf{p}, \mathbf{r}', \mathbf{p}', t), \quad (70)$$

where f_2 is a two-body distribution function, defined as an extension of Equation (67). This equation contains two unknown f and f_2 and hence cannot be solved as it stands.

If the system Hamiltonian H contains an interparticle interaction

$$V = \frac{1}{2} \int d^3 r \int d^3 r' v(\mathbf{r} - \mathbf{r}') \psi^\dagger(\mathbf{r}, t) \psi^\dagger(\mathbf{r}', t) \psi(\mathbf{r}', t) \psi(\mathbf{r}, t) \quad (71)$$

then the evolution equation for the field operator $\psi(\mathbf{r}, t)$ is nonlinear:

$$i\hbar \frac{\partial \psi(\mathbf{r}, t)}{\partial t} = \hbar \left(\mathbf{r}, -i\hbar \frac{\partial}{\partial \mathbf{r}} \right) \psi(\mathbf{r}, t) + \int d^3 r' \psi(\mathbf{r} - \mathbf{r}') \psi^\dagger(\mathbf{r}', t) \psi(\mathbf{r}, t). \quad (72)$$

In quantum field theory the basic dynamical variables are particle-field operators (ψ, ψ^\dagger) . The quantum statistics of the particles are given by the Bose commutation or the Fermi anticommutation rules satisfied by the field operators. The evolution equations of the field operators are intrinsically nonlinear when the interparticle interaction is present [10].

5.2. Phonons

Let us consider small oscillations for a system of atoms forming a SC lattice. Assume a longitudinal traveling wave along the x -axis. Imagine first hypothetical planes perpendicular to the x -axis containing atoms forming a square lattice. This plane has a mass per unit square of side length a (the lattice constant), equal to the atomic mass m . The plane is subjected to a restoring force per cm^2 equal to Young modulus Y . The dynamics of a set of the parallel planes is similar to that of coupled harmonic oscillators.

Assume next a transverse wave traveling along the x -axis. The hypothetical planes containing many atoms are subjected to a restoring stress equal to the shear modulus S . The dynamics is also similar to the coupled harmonic oscillators in 1D.

Low-frequency phonons are those to which Debye's continuum solid model [11] can be applied. The wave equations for the displacements $u(\mathbf{r}, t)$ are

$$\frac{\partial^2 u_i}{\partial t^2} = c_i^2 \nabla^2 u_i, \quad (73)$$

where $i = 1$ (longitudinal) or t (transverse). The longitudinal-wave phase velocity c_l is

$$c_l \equiv \sqrt{Y/\rho}, \quad (74)$$

where ρ is the mass density. The transverse-wave phase velocity c_t is

$$c_t \equiv \sqrt{S/\rho}, \quad (75)$$

The waves are superposable. Hence, phonons' travels are *not* restricted to the crystal's cubic directions. In short, there is a 3D k -vector, \mathbf{k} . The wave propagation is isotropic for each mode i .

Consider now the case of an ORC crystal. We may choose Cartesian coordinates (x, y, z) passing through the center of the unit cell. The small oscillations are similar to the case of a SC lattice. The dynamics of the parallel plates are the same but the restoring forces are different in x -, y - and z -directions. The plane waves have different phase velocities, depending on the directions. They are superposable since these waves are still solutions of the wave Equations (73).

Phonons are quanta corresponding to the running plane-wave modes of lattice vibrations. Phonons are bosons, and the energies are distributed, following the Planck distribution function:

$$f(\varepsilon) = [\exp(\varepsilon/k_B T) + 1]^{-1}. \quad (76)$$

There is no activation energy unlike the case of the “electrons”. This arises from the boson nature of phonons. The temperature T alone determines the average number and energy.

Phonons and conduction electrons are generated based on the same lattice and k -space. This is important when describing the electron-phonon interaction.

The “electrons” and “holes” have the same orthogonal unit cell size. The average phonon size is much greater than the electron size. The low-energy phonons have small k and great wavelengths. The average energy of a fermionic electron is greater than a bosonic phonon by two or more orders of magnitude. This establishes a usual physical picture that a point-like electron runs, and is occasionally scattered by a cloud-like phonon in the crystal.

We saw earlier that a MCL crystal has 1D k -vectors pointing along the c -axis for the electrons. There are similar 1D k -vectors for phonons. Besides, there are two other sets of 1D k -vectors. Plane waves running in the z -direction can be visualized by imagining the parallel plates, each containing a great number of atoms executing *longitudinal* and *transverse* small oscillations. Consider an oblique net of points (atoms) viewed from

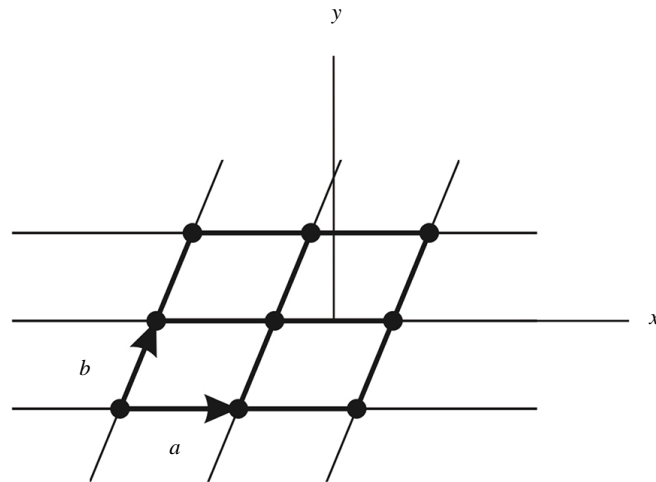


Figure 4. An oblique net with base vectors (a, b) .

the top, shown in **Figure 4**. Planes defined by the vector \mathbf{a} and the c -axis are parallel and each plane contains a great number of atoms. Planes defined by the vector \mathbf{b} and the c -axis are also parallel, and each contains a number of atoms also executing small oscillations. These three sets of 1D phonons stabilize the lattice. The phonons run anisotropically since the restoring stresses and phase velocities are direction-dependent.

We next consider a TCL crystal, which has no k -vectors for the electrons. There are, however, a set of 1D k -vectors for phonons. Take a primitive TCL unit cell. The opposing faces are parallel to each other. There are restoring forces characterized by Young modulus Y and shear modulus S . Then, there are 1D k -vectors perpendicular to the faces. The set of 1D phonons can stabilize the lattice. These phonons in TCL are highly directional. There is no spherical wave formed.

We used the lattice property that the facing planes are parallel. This parallel-plane configuration is common to all seven crystal systems [1] [12]. A typical HEX system, graphite, clearly has three sets of parallel material planes containing many atoms. The RHL system has parallel planes, too. The parallel material planes configuration is the basic condition for the phonon generation and the lattice stability.

5.3. Metal-Insulator Transition

In 1959 Morin reported his discovery of a metal-insulator transition (MIT) in vanadium dioxide (VO_2) [13]. Compound VO_2 forms a monoclinic (MCL) crystal on the low temperature side and a tetragonal (TET) crystal on the high temperature side. When heated, VO_2 undergoes an insulator-to-metal transition around 340 K, with the resistance drop by four orders of magnitude. The origin of the phase transition has been attributed to Peierls instability driven by strong electron-phonon interaction [14], or to Coulomb repulsion and electron localization due to the electron-electron interaction on a Mott-Hubbard picture by other authors [15]-[17].

A simpler view on the MIT we propose is as follows [18]. The existence of k -vectors is prerequisite for the electrical conduction. The TET (VO_2)₃ unit cells are periodic along the crystal's x -, y -, and z -axes, and hence there are three-dimensional (3D) k -vectors. There are 1D k -vectors along the c -axis for a MCL crystal. The MIT occurs since the dimensionality of the k -vectors is reduced from three (3) to one (1) is going from the TET to the MCL crystals.

Whittaker *et al.* [19] measured the resistance R in K-doped V_2O_5 nanowires. They observed that (a) the resistance R for the low-temperature (MCL) phase shows an Arrhenius-type T -dependence:

$$\sigma \propto R^{-1} \propto \exp(-\varepsilon_a/k_B T) \quad (77)$$

ε_a = activation energy (≈ 300 eV), k_B = Boltzmann constant, and that (b) the resistance R for the high-temperature (TET) phase is T -independent. These different behaviors may arise as follows: the currents in (a) run along the nanowire axis, which is also the easy c -axis of the MCL crystal. Hence the Arrhenius behavior (for the conductivity) is observed for the case (a). For the case (b) the currents run in 3D. Only those electrons near the Fermi surface are excited and participate in the transport. Then, the density of excited electrons, n_x , is related to the total electron density n_0 by

$$n_x = \alpha n_0 \frac{k_B T}{\varepsilon_a}, \quad (78)$$

where α is a number close to unity. The factor T drops out with the T -linear phonon scattering rate (for the conductivity). The T -dependence of the exponential factor is small since the activation energy ε_a is much greater than the observation temperature around 10°C. Thus, the resistance is nearly constant. There is a sudden drop of resistance around 300 K, where the two phases separate.

The MIT designation is a misnomer. The semiconductor-microconductor transition correctly describes the phenomenon since the transition is between the 3D- k semiconductor with an activation energy and the 1D- k semiconductor called here the microconductor. In the low temperature phase the resistance R decreases with the temperature T , indicating the semiconductor character. In the normal metal the resistance R increases with T , arising from the phonon population change. In the high temperature phase the resistance R is finite, and therefore the material is not insulator. There are sharp drop and rise in the resistance, and the phase change depends on the heating and cooling directions, arising from the domain-by-domain transitions.

5.4. Graphene

Graphene forms a 2D honeycomb lattice. The WS unit cell is a rhombus (darkened area) shown in **Figure 5(a)**. We showed in our earlier work [18] that the graphene has “electrons” and “holes” based on the rectangular unit cell (dotted black-lines) shown in **Figure 5(b)**. We briefly review our calculations.

The prevalent theory based on the WS rhombus unit cell model predicts a gapless semiconductor with an “electron”-“hole” symmetry. In our earlier work [18] we showed that (a) the “electron” and the “hole” have different charge distributions and different effective masses, (b) that the “electrons” and “holes” move in different easy channels, (c) that the “electrons” and “holes” are thermally excited with different activation energies, and (d) that the “electron” activation energy ε_1 is smaller than the “hole” activation energy ε_2 :

$$\varepsilon_1 < \varepsilon_2. \quad (79)$$

Thus, “electrons” are the majority carriers in graphene. The thermally activated electron densities are then given by

$$n_j(T) = n_j e^{-\varepsilon_j/k_B T}, \quad n_j = \text{constant}, \quad (80)$$

where $j=1$ and 2 represent the “electron” and “hole”, respectively. Magnetotransport experiments by Zhang *et al.* [20] indicate that the “electrons” are majority carriers in graphene. Thus, our theory is in agreement with experiments.

5.5. Graphite

Graphite is composed of graphene layers stacked in the manner ABAB... along the c -axis. We may choose an orthogonal (Cartesian) unit cell shown in **Figure 6**. The unit cell contains 16 C's. The two rectangles (white solid lines) are stacked vertically with the interlayer separation, $c_0 = 3.35 \text{ \AA}$ much greater than the nearest neighbor distance between two C's, $a_0 = 1.42 \text{ \AA}$:

$$c_0 \gg a_0. \quad (81)$$

The unit cell has three side-lengths:

$$b_1 = 3a_0, \quad b_2 = 2\sqrt{3}a_0, \quad b_3 = 2c_0. \quad (82)$$

Clearly, the system is periodic along the orthogonal directions with the three periods (b_1, b_2, b_3) given in

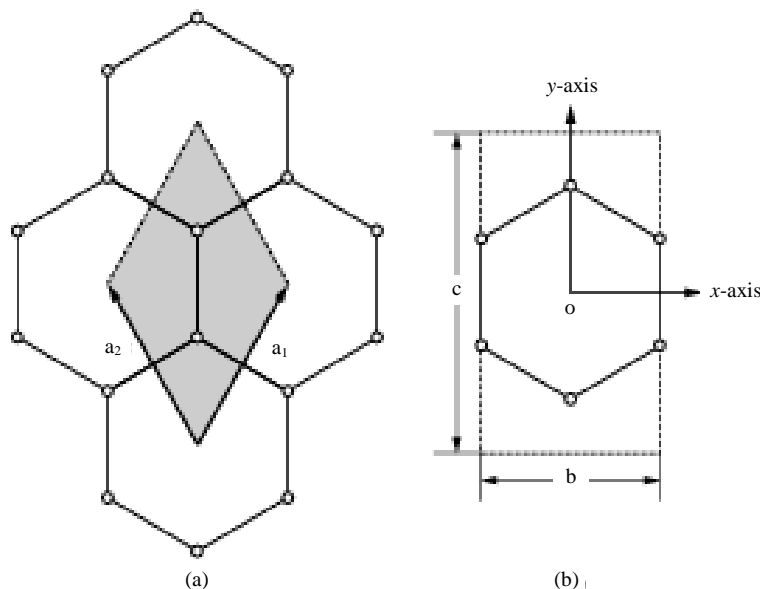


Figure 5. (a) WS unit cell, rhombus (darkened area) for graphene; (b) The orthogonal unit cell, rectangle (dotted lines).

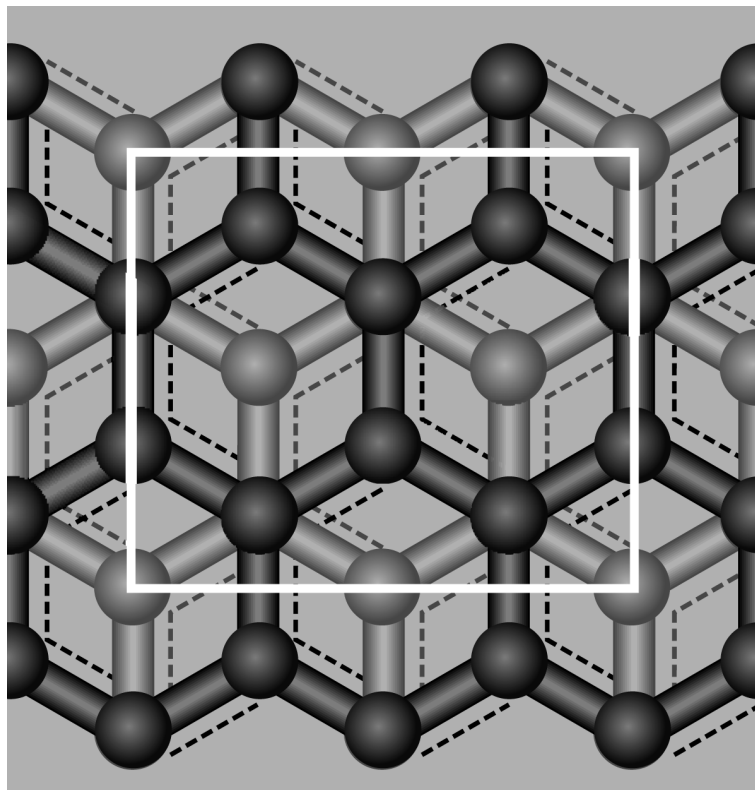


Figure 6. An orthogonal (Cartesian) unit cell (white solid lines) viewed from the top for graphite. The unit cell of graphite has two layers of graphene. The carbons (circles) in the A (B) planes are shown in black (gray).

Equation (82). Both “electron” and “hole” have the same unit cell size. The system is orthorhombic with the sides (b_1, b_2, b_3) , $b_1 \neq b_2$, $b_1 \neq b_3$, $b_2 \neq b_3$.

The negatively charged “electron” (with the charge $-e$) in graphite is welcomed by the positively charged C^+ when moving vertically up or downwards on the paper. That is, the easy directions for the “electrons” are vertical. The easy directions for the “holes” are horizontal. There are no hindering hills for “holes” moving horizontally. Hence, the “electron” in graphite has the lower activation energy than the “hole”: $\varepsilon_1 < \varepsilon_2$. Then, “electrons” are the majority carriers in graphite. The thermoelectric power (Seebeck coefficient) measurements by Kang *et al.* [21] show that the majority carriers in graphite are “electrons”, in agreement with our theory.

It is sometimes said [22] that since the separation distance c_0 is much greater than the nearest neighbor distance a_0 , the conduction in graphite is two-dimensional, and can be discussed in terms of the motion in the graphene as a first approximation. We take a different point of view. The conduction electrons move as wave packets having the 3D orthogonal unit cell sizes. The conduction is two-dimensional because of the inequality (81). But the transport behaviors in graphite and graphene are very different because of the different unit cells. A room temperature quantum Hall effect (QHE) was observed in graphene [23] [24]. Are there quantum Hall and superconductivity states for graphite, too? These are important questions.

The construction of the orthogonal unit cell developed here can be followed in other materials forming HEX crystals: Zinc (Zn) and Beryllium (Be) form HEX crystals. The closed orbits on the coronet-like Fermi surface generate cyclotron resonance, which may be discussed using the orthogonal unit cells.

6. Summary

In summary, we established that

- The conduction electron (“electron”, “hole”) in an ORC crystal moves when a primitive orthogonal unit cell is chosen as the quantum wave packet.

- CUB, TET, ORC, RHL, HEX crystal systems have 3D k -spaces for electrons. The MCL system has a 1D k -space. The TCL has no k -vectors.
- The MCL and TCL have 1D phonons, which are highly directional. No spherical phonon distributions are generated.
- For RHL and HEX crystals the orthogonal unit cells different from the WS unit cells must be chosen for electron and phonon dynamics.
- “Electrons” and “holes” have the same unit cell size, and they move with different effective masses. “Electrons” and “holes” in semiconductors are excited with different activation energies. Phonons are excited with no activation energies.
- Both phonons and electrons are generated based on the same orthogonal unit cells. This fact is important when dealing with the electron-phonon interaction.
- The electron size is the primitive unit cell size. The average phonon size is greater by two or more orders of magnitude at the room temperature.
- Instantaneous interparticle Coulomb potential $V(r) = kq/r$ violates the special relativity principles. Dirac’s theorem [2] about interparticles (electrons) as wave packets is valid if the Coulomb interaction is described in relativistic quantum field theory, and it is regarded as a result of a longitudinal photon exchange between the electrons.
- The MIT in VO_2 is in reality a transition between two semiconductors having 1D and 3D k -vectors. The 1D semiconductor (low temperature phase) is highly anisotropic.
- The majority carriers in graphene and graphite are “electrons”.
- Graphite has “electrons” and “holes”. Phonon exchange may generate Cooper pairs. Then graphite can be a superconductor.

References

- [1] Ashcroft, N.W. and Mermin, N.D. (1976) *Solid State Physics*. Saunders College, Philadelphia, 116, 217.
- [2] Dirac, P.A.M. (1958) *Principles of Quantum Mechanics*. 4th Edition, Oxford University Press, London, 121-125. <http://dx.doi.org/10.1063/1.3062610>
- [3] Ehrenfest, P. (1927) *Zeitschrift für Physik*, **45**, 455-457. <http://dx.doi.org/10.1007/BF01329203>
- [4] Bloch, F. (1928) *Zeitschrift für Physik*, **52**, 555-600. <http://dx.doi.org/10.1007/BF01339455>
- [5] Kronig, R.L. and Penney, W.G. (1931) *Proceedings of the Royal Society of London*, **130**, 499. <http://dx.doi.org/10.1098/rspa.1931.0019>
- [6] Wigner, E. and Seitz, F. (1933) *Physical Review*, **43**, 204.
- [7] Drude, P. (1900) *Annalen der Physik*, **1**, 566; **3**, 369.
- [8] Haug, A. (1972) *Theoretical Solid-State Physics*, Vol. 1. Pergamon, Oxford, 64-69.
- [9] Shukla, K. (1990) *Kronig-Penney Models and Their Applications to Solids*. Ph.D. Thesis, State University of New York at Buffalo.
- [10] Fujita, S., McNabb III, J. and Suzuki, A. (2014) *Journal of Modern Physics*, **5**, 171. <http://dx.doi.org/10.4236/jmp.2014.55027>
- [11] Debye, P. (1912) *Annalen der Physik*, **39**, 789-839. <http://dx.doi.org/10.1002/andp.19123441404>
- [12] Kittel, C. (1986) *Introduction to Solid State Physics*. 6th Edition, John Wiley & Sons, Inc., New York, 10-12.
- [13] Morin, F.J. (1959) *Physical Review Letters*, **3**, 34-36. <http://dx.doi.org/10.1103/PhysRevLett.3.34>
- [14] Goodenough, J.B. (1971) *Journal of Solid State Chemistry*, **3**, 490-500. [http://dx.doi.org/10.1016/0022-4596\(71\)90091-0](http://dx.doi.org/10.1016/0022-4596(71)90091-0)
- [15] Mott, N.F. (1968) *Reviews of Modern Physics*, **40**, 677-683. <http://dx.doi.org/10.1103/RevModPhys.40.677>
- [16] Wentzcovitch, R.M., Schulz, W.W. and Allen, P.B. (1994) *Physical Review Letters*, **72**, 3389-3392. <http://dx.doi.org/10.1103/PhysRevLett.72.3389>
- [17] Rice, T.M., Launois, H. and Pouget, J.P. (1994) *Physical Review Letters*, **73**, 3042. <http://dx.doi.org/10.1103/PhysRevLett.73.3042>
- [18] Fujita, S., Jovaini, A., Godoy, S. and Suzuki, A. (2012) *Physics Letters A*, **376**, 2808-2811. <http://dx.doi.org/10.1016/j.physleta.2012.08.027>
- [19] Whittaker, L., Patridge, C.J. and Banerjee, S. (2011) *The Journal of Physical Chemistry Letters*, **2**, 745-758.

<http://dx.doi.org/10.1021/jz101640n>

- [20] Zhang, Y., Tan, Y.W., Stormer, H.L. and Kim, P. (2005) *Nature*, **438**, 201-204. <http://dx.doi.org/10.1038/nature04235>
- [21] Kang, N., Lu, L., Kong, W.J., Hu, J.S., Yi, W., Wang, Y.P., Zhang, D.J., Pan, Z.W. and Xie, S.S. (2003) *Physical Review B*, **67**, Article ID: 033404. <http://dx.doi.org/10.1103/PhysRevB.67.033404>
- [22] Saito, R., Dresselhaus, G. and Dresselhaus, M.S. (1998) *Physical Properties of Carbon Nanotubes*. Imperial College Press, London, 25. <http://dx.doi.org/10.1142/9781860943799>
- [23] Novoselov, K.S., Geim, A.K., Morozov, S.V., Jiang, D., Katsnelson, M.I., Grigorieva, I.V., Dubonos, S.V. and Firsov, A.A. (2005) *Nature*, **438**, 197-200. <http://dx.doi.org/10.1038/nature04233>
- [24] Novoselov, K.S., Jiang, Z., Zhang, Y., Morozov, S.V., Stormer, H.I., Zeitler, U., Maan, J.C., Boebinger, G.S., Kim, P. and Geim, A.K. (2007) *Science*, **315**, 1379. <http://dx.doi.org/10.1126/science.1137201>